A moving Kriging interpolation-based boundary node method for two-dimensional potential problems*

Li Xing-Guo(李兴国), Dai Bao-Dong(戴保东)†, and Wang Ling-Hui(王灵卉)

Department of Engineering Mechanics, Taiyuan University of Science & Technology, Taiyuan 030024, *China*

(Received 28 June 2010; revised manuscript received 5 August 2010)

In this paper, a meshfree boundary integral equation (BIE) method, called the moving Kriging interpolation-based boundary node method (MKIBNM), is developed for solving two-dimensional potential problems. This study combines the BIE method with the moving Kriging interpolation to present a boundary-type meshfree method, and the corresponding formulae of the MKIBNM are derived. In the present method, the moving Kriging interpolation is applied instead of the traditional moving least-square approximation to overcome Kronecker's delta property, then the boundary conditions can be imposed directly and easily. To verify the accuracy and stability of the present formulation, three selected numerical examples are presented to demonstrate the efficiency of MKIBNM numerically.

Keywords: meshfree method, moving Kriging interpolation method, boundary integral equation, boundary node method, potential problem

PACC: 0260, 0270, 1240Q

1. Introduction

In recent years, the meshfree (or meshless) method, which has achieved remarkable progress in computational mechanics and related fields, has received more and more attention due to its flexibility and good convergence rate.[1,2] Beyond the traditional finite element method (FEM), mesh is not necessary in the meshfree method, then the large deformation, fracture mechanics with crack growth and explosion problems can be simulated with the method without re-meshing technique. A group of meshfree methods have been proposed in recent years and applied in engineering computation. Nayroles *et al.* have developed an important step towards the meshfree method, called the diffuse element method (DEM).[3] Belytschko *et al.* have refined and modified the DEM to formulate the so-called element-free Garlerkin (EFG) method.[4] Atluri *et al.* have proposed a meshless local Petrov–Galerkin (MLPG) method.[5] There are also other meshfree methods which have been developed and applied in engineering computation, such as the point interpolation method,[6] the complex variable meshless method,[7,8] reproducing kernel particle method with complex variables,[9,10] hybrid boundary node method,[11] the boundary element-free method (BEFM).[12−17]

The boundary element method (BEM) is a numerical technique based on boundary integral equation, which has been developed since the middle of the last century. A key feature of the BEM is that it only requires discretization of the surface rather than volume. In other words, only the two-dimensional (2D) bounding surface of a three-dimensional (3D) body needs to be discretized. Combining the moving least-square (MLS) approximation[18] with boundary integral equation (BIE) method, Mukherjee *et al.* have presented a meshfree method of the BIE to solve potential problems and linear elasticity problems, called the boundary node method (BNM).[19,20] Atluri *et al.* have developed another important meshfree method, called the local boundary integral equation (LBIE) method to solve the linear and nonlinear boundary value problems.[21,22] The BNM does not require element or mesh for the interpolation of boundary variables and possesses the advantage of dimensionality

*Project supported by the Young Scientists Fund of the National Natural Science Foundation of China (Grant No. 10902076), the Natural Science Foundation of Shanxi Province of China (Grant No. 2007011009), the Scientific Research and Development Program of the Shanxi Higher Education Institutions (Grant No. 20091131), and the Doctoral Startup Foundation of Taiyuan University of Science and Technology (Grant No. 200708).

†Corresponding author. E-mail: Dai_baodong@126.com

reduction. However, the boundary conditions cannot be satisfied accurately because the shape functions based on MLS approximation lack Kronecker's delta property. The LBIE method can easily solve a complicated boundary value problem, but the local foundational solution is more complicated than that the conventional BEM uses.

The Kriging interpolation is a form of generalized linear regression for the formulation of an optimal estimator in a minimum mean square error sense. Gu[23] has first introduced the moving Kriging interpolation and has successfully demonstrated the effectiveness of the moving Kriging interpolation functions in solving one-dimensional (1D) steady-state heat conduction problems. Combining the BIE method with the moving Kriging interpolation, the moving Kriging interpolation-based boundary node method (MKIBNM) is proposed in this paper. The moving Kriging interpolation based on a group of arbitrarily distributed points on the boundary of the problem domain is adopted to construct the shape functions.[23,24] Because the shape functions possess Kronecker's delta property, the MKIBNM overcomes the shortcomings of BNM. The boundary conditions can be imposed as the conventional BEM.

An implementation of the MKIBNM has been presented for 2D potential problems in the rest of this paper. Several numerical examples are presented to demonstrate the method.

2. Moving Kriging

2.1. Moving Kriging interpolation

The moving Kriging interpolation in the MKIBNM are defined on the 1D bounding surface of 2D domain Ω, using a set of discrete nodes on Γ. As in the conventional BEM formulation, the moving Kriging interpolation for u and q can be constructed independently.

Consider a sub-domain $\Gamma_x \subseteq \Gamma$, the neighbourhood of a point s, in which the total number of the nodes is n. The Kriging interpolation for u and its normal derivative $q \equiv \partial u/\partial n$ on Γ are defined as follows:

$$\boldsymbol{u}^{\mathrm{h}}(s) = [\boldsymbol{p}^{\mathrm{T}}(s)\boldsymbol{S}_\alpha + \boldsymbol{r}^{\mathrm{T}}(s)\boldsymbol{S}_\beta]\boldsymbol{U}, \tag{1}$$

$$\boldsymbol{q}^{\mathrm{h}}(s) = [\boldsymbol{p}^{\mathrm{T}}(s)\boldsymbol{S}_\alpha + \boldsymbol{r}^{\mathrm{T}}(s)\boldsymbol{S}_\beta]\boldsymbol{Q}, \tag{2}$$

where s is a curvilinear coordinate (here the arc length) on Γ. Unlike Cartesian coordinates, in the present work, s is chosen to be the local coordinate of a boundary point with respect to the evaluation point. For example, the value of s for an evaluation point is always zero, points lying 'ahead' of the evaluation point have positive values of s while those 'behind' it have the negative values of s. $p_j(s) = [\,1 \;\; s \;\cdots\; s^{m-1}\,]$ are monomial basis function in s. Matrices $\boldsymbol{S}_\alpha$ and $\boldsymbol{S}_\beta$ are

$$\boldsymbol{S}_\alpha = (\boldsymbol{P}^{\mathrm{T}}\boldsymbol{R}^{-1}\boldsymbol{P})^{-1}\boldsymbol{P}^{\mathrm{T}}\boldsymbol{R}^{-1}, \tag{3}$$

and

$$\boldsymbol{S}_\beta = \boldsymbol{R}^{-1}(\boldsymbol{I} - \boldsymbol{P}\boldsymbol{S}_\alpha), \tag{4}$$

where $\boldsymbol{I}$ is a unit matrix.

The $n \times m$ matrix $\boldsymbol{P}$ that has evaluated function values at the given set of nodes is defined as

$$\boldsymbol{P} = \begin{bmatrix} \boldsymbol{p}(s_1) \\ \vdots \\ \boldsymbol{p}(s_n) \end{bmatrix} = \begin{bmatrix} p_1(s_1) & p_2(s_1) & \cdots & p_m(s_1) \\ p_1(s_2) & p_2(s_2) & \cdots & p_m(s_2) \\ \vdots & \vdots & \ddots & \vdots \\ p_1(s_n) & p_2(s_n) & \cdots & p_m(s_n) \end{bmatrix}. \tag{5}$$

And the $n \times n$ matrix of correlation $\boldsymbol{R}$ is given in an explicit form

$$\boldsymbol{R}[R(s_i, s_j)] = \begin{bmatrix} 1 & R(s_1, s_2) & \cdots & R(s_1, s_n) \\ R(s_2, s_1) & 1 & \cdots & R(s_2, s_n) \\ \vdots & \vdots & \ddots & \vdots \\ R(s_n, s_1) & R(s_n, s_2) & \cdots & 1 \end{bmatrix}. \tag{6}$$

The $r(s)$ in Eqs. (1) and (2) is also given as

$$\boldsymbol{r}(s) = [R(s, s_1) \quad R(s, s_2) \quad \cdots \quad R(s, s_n)]^{\mathrm{T}}, \tag{7}$$

where $R(s_i, s_j)$ is the correlation function between any two of the n nodes s_i and s_j. There exist various functions that could be selected, however, a frequently and widely used one is Gaussian function

$$R(s_i, s_j) = \exp(-\eta r_{ij}^2), \tag{8}$$

where

$$r_{ij} = \|s_i - s_j\|, \tag{9}$$

and $\eta > 0$ is a correlation parameter of the model.

Equations (1) and (2) can also be rewritten as

$$u^h(s) = \boldsymbol{\Phi}(s)\boldsymbol{U} = \sum_k^n \phi_k(s)u_k, \tag{10}$$

$$q^{\mathrm{h}}(s) = \boldsymbol{\Phi}(s)\boldsymbol{Q} = \sum_k^n \phi_k(s)q_k, \tag{11}$$

where $\phi_k(s)$ is the moving Kriging shape function associated with node k, defined by

$$\phi_k(s) = \sum_{j=1}^{m} p_j(s) S_{\alpha jk} + \sum_{i=1}^{n} r_k(s) S_{\beta ik}. \tag{12}$$

The 1D shape functions with $p(s) = \{1, s, s^2\}$ are shown in Fig. 1. It can be found that Kronecker's delta property is satisfied.

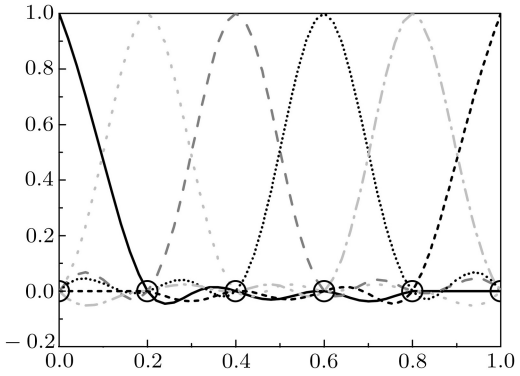

Fig. 1. The 1D shape functions with $p(s) = \{1, s, s^2\}$.

2.2. Mathematical properties of moving Kriging interpolation

A key property of the moving Kriging shape function is the Kronecker's delta property. It leads to a simple procedure of implementation of boundary conditions. The moving Kriging shape function in Eq. (12) can also be rewritten in other form at the node $s = s_i$ with $i = 1, 2, \ldots, n$

$$\phi_k(s_i) = \sum_{j=1}^{m} p_j(s_i) S_{\alpha jk} + \sum_{i=1}^{n} r_k(s_i) S_{\beta ik}, \tag{13}$$

which can be written in the form

$$[\phi_k(s_i)] = \boldsymbol{P}\boldsymbol{S}_\alpha + \boldsymbol{R}\boldsymbol{S}_\beta, \tag{14}$$

where $\boldsymbol{S}_\alpha$, $\boldsymbol{S}_\beta$, $\boldsymbol{P}$, and $\boldsymbol{R}$ are given by Eqs. (3)–(6), respectively. Substituting Eqs. (3) and (4) into Eq. (14) leads to

$$[\phi_k(s_i)] = \boldsymbol{P}\boldsymbol{S}_\alpha + \boldsymbol{R}\boldsymbol{R}^{-1}(\boldsymbol{I} - \boldsymbol{P}\boldsymbol{S}_\alpha) = \boldsymbol{I} \tag{15}$$

or

$$\phi_k(s_j) = \begin{cases} 1 \ (k = j; k, j = 1, 2, \ldots, n), \\ 0 \ (k \neq j; k, j = 1, 2, \ldots, n). \end{cases} \tag{16}$$

Another important property of the moving Kriging shape functions is that the moving Kriging interpolation can reproduce any function in the basis exactly.[23] In particular, if a linear basis is employed to construct the moving Kriging shape functions, all constants and linear terms can then be reproduced exactly, i.e.

$$\sum_{k=1}^{n} \phi_k(s) = 1, \tag{17}$$

$$\sum_{k=1}^{n} \phi_k(s) s_k = s. \tag{18}$$

3. MKIBNM formulation

Consider the following 2D potential problem in the domain Ω bounded by Γ

$$\begin{cases} \nabla^2 u(\boldsymbol{x}) = 0 & \text{in } \Omega, \\ u(\boldsymbol{x}) = \bar{u}(\boldsymbol{x}) & \boldsymbol{x} \in \Gamma_u, \\ q(\boldsymbol{x}) = \dfrac{\partial u(\boldsymbol{x})}{\partial n} = \bar{q}(\boldsymbol{x}) & \boldsymbol{x} \in \Gamma_t, \end{cases} \tag{19}$$

where $u(\boldsymbol{x})$ is an unknown function, and n is the normal to the boundary Γ.

The well-known BIE formulation for 2D potential problems is given by

$$C(\boldsymbol{\xi})u(\boldsymbol{\xi}) = \int_\Gamma u^*(\boldsymbol{\xi}, \boldsymbol{x}) q(\boldsymbol{x}) \mathrm{d}\Gamma - \int_\Gamma \frac{\partial u^*(\boldsymbol{\xi}, \boldsymbol{x})}{\partial n} u(\boldsymbol{x}) \mathrm{d}\Gamma, \tag{20}$$

where $C(\boldsymbol{\xi})$ is a coefficient which depends on the internal angle the boundary Γ makes at the given source point ξ. The value of $C(\boldsymbol{\xi})$ for any boundary can be proved to be $C(\boldsymbol{\xi}) = \theta/2\pi$, where θ is the internal angle of the corner in radians. In addition, when the source point ξ is located inside the domain Ω, $C(\boldsymbol{\xi}) = 1$; and u^* is the fundamental solution for potential problems. The fundamental solution for 2D potential problems is given by

$$u^*(\boldsymbol{\xi}, \boldsymbol{x}) = \frac{1}{2\pi} \ln \frac{1}{r(\boldsymbol{\xi}, \boldsymbol{x})}, \tag{21}$$

where $r(\boldsymbol{\xi}, \boldsymbol{x})$ is the distance between the source point $\boldsymbol{\xi}$ and the field point $\boldsymbol{x}$.

The boundary Γ is assumed to be divided into sub-domains Γ_i, $(i = 1, 2, \ldots, N)$, with N being the total number of the sub-domains. Γ_i and Γ_{i-1} are connected with a point, and Γ_i is only used to carry out numerical integration in Eq. (20).

Equation (20) can also be rewritten as

$$C(\xi)u(\xi) = \sum_{i=1}^{N} \int_{\Gamma_i} u^*(\xi, \boldsymbol{x}) \frac{\partial u(\boldsymbol{x})}{\partial n} \mathrm{d}\Gamma - \sum_{i=1}^{N} \int_{\Gamma_i} \frac{\partial u^*(\xi, \boldsymbol{x})}{\partial n} u(\boldsymbol{x}) \mathrm{d}\Gamma. \tag{22}$$

Substituting Eqs. (10) and (11) into Eq. (22) yields the following equation

$$C(\xi_n)u(\xi_n) = \sum_{i=1}^{N} \int_{\Gamma_i} u^*(\xi_n, \boldsymbol{x}) \sum_{k=1}^{n_k} \phi_k(\boldsymbol{x}) q(\xi_k) \mathrm{d}\Gamma - \sum_{i=1}^{N} \int_{\Gamma_i} \frac{\partial u^*(\xi_n, \boldsymbol{x})}{\partial n} \sum_{k=1}^{n_k} \phi_k(\boldsymbol{x}) u(\xi_k) \mathrm{d}\Gamma, \tag{23}$$

where ξ_n is the source point and n_k is the number of boundary nodes in the domain depending on the field point $\boldsymbol{x}$.

Equation (23) can be written as

$$C(\xi_n)u(\xi_n) = \sum_{i=1}^{N} \sum_{k=1}^{n_k} q(\xi_k) \int_{-1}^{1} u^*(\xi_n, \boldsymbol{x}) \phi_k(\boldsymbol{x}) J(\eta) \mathrm{d}\eta - \sum_{i=1}^{N} \sum_{k=1}^{n_k} u(\xi_k) \int_{-1}^{1} q^*(\xi_n, \boldsymbol{x}) \phi_k(\boldsymbol{x}) J(\eta) \mathrm{d}\eta, \tag{24}$$

where η is the local coordinate and $J(\eta)$ is the Jacobian.

$$J(\eta) = \sqrt{\left(\frac{\mathrm{d}x}{\mathrm{d}\eta}\right)^2 + \left(\frac{\mathrm{d}y}{\mathrm{d}\eta}\right)^2}. \tag{25}$$

Using the numerical method for the integrals in Eq. (24) to every source point, we can obtain the MKIBNM system equation

$$\boldsymbol{CU} + \boldsymbol{HU} = \boldsymbol{GQ}, \tag{26}$$

where

$$\boldsymbol{U} = [u(\boldsymbol{x}_1) \quad u(\boldsymbol{x}_2) \quad \ldots \quad u(\boldsymbol{x}_N)]^{\mathrm{T}}, \tag{27}$$

$$\boldsymbol{Q} = [q(\boldsymbol{x}_1) \quad q(\boldsymbol{x}_2) \quad \ldots \quad q(\boldsymbol{x}_N)]^{\mathrm{T}}, \tag{28}$$

and $\boldsymbol{C}$, $\boldsymbol{H}$, and $\boldsymbol{G}$ are the corresponding coefficient matrices.

We can see that the integrands in Eq. (24) include some log singular integrals, the singular integrals are evaluated by the logarithmic Gaussian quadrature formulation.

Because the shape functions of MKIBNM have Kronecker's delta property, the boundary conditions can be implemented in the same way as the conventional BEM. Substituting the boundary conditions into Eq. (26) and solving the system equation, we can obtain all the unknown boundary node values. It is possible to calculate any internal value of u, the value of u is calculated at any internal point using Eq. (24), which can be rewritten as

$$u(\xi) = \sum_{i=1}^{N} \int_{\Gamma_i} u^*(\xi, \boldsymbol{x}) \frac{\partial u(\boldsymbol{x})}{\partial n} \mathrm{d}\Gamma - \sum_{i=1}^{N} \int_{\Gamma_i} \frac{\partial u^*(\xi, \boldsymbol{x})}{\partial n} u(\boldsymbol{x}) \mathrm{d}\Gamma. \tag{29}$$

This is the MKIBNM for 2D potential problems.

4. Numerical examples

In this section, three examples are presented to demonstrate the applicability of the MKIBNM for 2D potential problems. It must be pointed out that the linear basis function is used in the MKIBNM, and the correlation function is a Gaussian function with the correlation parameter $\eta = 10$. The numerical results obtained by the MKIBNM are compared with the exact solutions for showing the effectiveness of the present method.

4.1. Modified Neumann problem of a circle

We consider a modified Neumann problem for a circle with radius $r_0 = 3$, the prescribed boundary conditions are

$$q = \frac{\mathrm{d}u}{\mathrm{d}n} = \cos\theta$$

except for the points (3, 0) and (3, π) (the ends of the horizontal diameter), where $u\,|_{\theta=0} = 3$, and $u\,|_{\theta=\pi} = -3$, θ is the usual polar coordinate.

The exact solution of this problem is

$$u(r, \theta) = x = r_0 \cos\theta,$$

The circular plate shown in Fig. 2 is considered here, a total of 32 boundary nodes are used to discretize the boundary of the problem. The 32 uniform integration cells are employed to evaluate the integral of matrices.

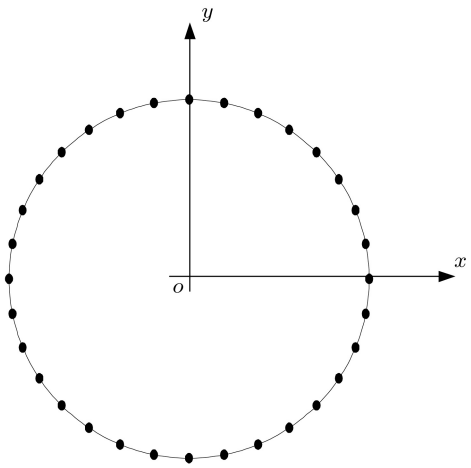

Fig. 2. Node distribution.

Numerical results from the MKIBNM, together with the exact solution are shown in Fig. 3. It is evident that the results accord well with the exact solution.

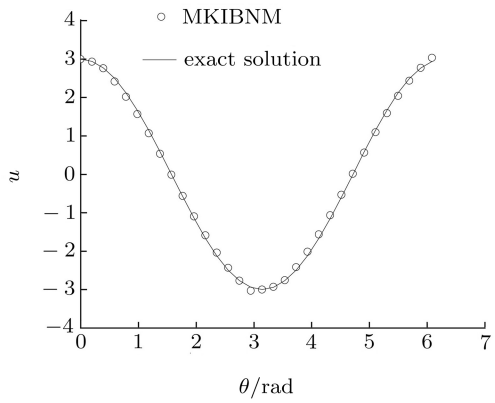

Fig. 3. Exact and numerical solutions of u at the boundary.

4.2. Dirichlet problem of an ellipse

The second example we consider is a Dirichlet problem of an ellipse. The ellipse has the equation

$$x = a\cos\theta, \quad y = b\sin\theta.$$

In this example, we set $a = 5000$, $b = 2500$. The prescribed boundary conditions are $u = x = a\cos\theta$.

The exact solution of this problem is

$$q = \frac{b^2 x}{\sqrt{a^4 y^2 + b^4 x^2}} = \frac{b^2\cos\theta}{\sqrt{a^2\sin^2\theta + b^2\cos^2\theta}}.$$

The elliptic plate shown in Fig. 4 is considered here, a total of 48 boundary nodes are used to discretize the boundary of the problem. The 48 uniform integration cells are used to evaluate the integral of matrices.

Numerical results from the MKIBNM, together with the exact solution, are shown in Fig. 5. It can be seen that the present results are in excellent agreement with the exact solution.

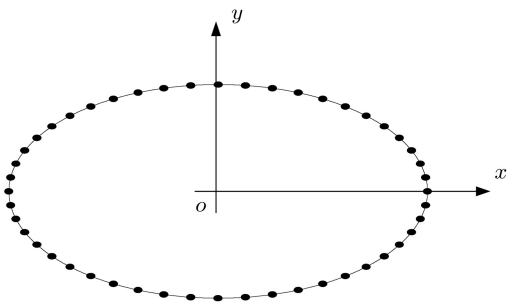

Fig. 4. Node distribution.

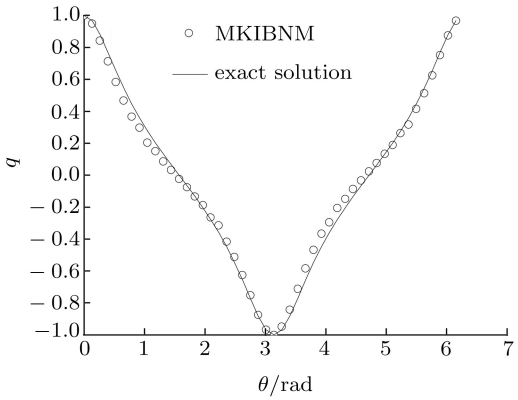

Fig. 5. Exact and numerical solutions of u at the boundary.

4.3. Mixed problem of a square

The third example we consider is a mixed problem for a square. The rectangular plate is governed by Laplace equation

$$\nabla^2 u(\boldsymbol{x}) = 0, \quad x \in [0,5], \quad y \in [0,10].$$

The prescribed boundary conditions are

$$u(0,y) = 0, \quad \frac{\partial u(5,y)}{\partial x} = 0,$$

$$u(x,10) = 100\sin(\pi x/10), \quad u(x,0) = 0.$$

The exact solution for u is

$$u(x,y) = \frac{100\sin(\pi x/10)\sinh(\pi y/10)}{\sinh(\pi)}.$$

The rectangular plate shown in Fig. 6 is considered, a total of 60 boundary nodes are used to discretize the boundary of the problem. The 60 uniform

integration cells are used to evaluate the integral of matrices.

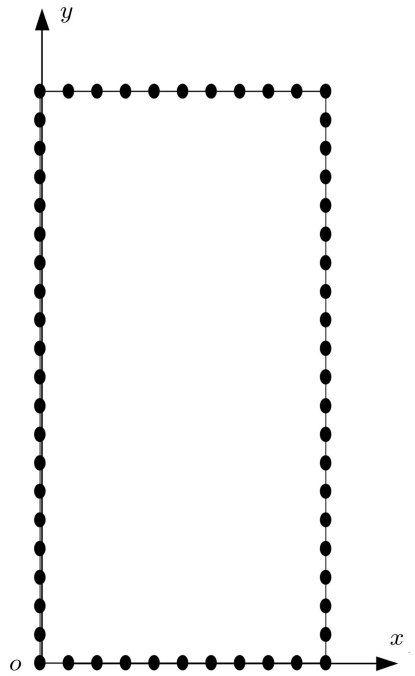

Fig. 6. Node distribution.

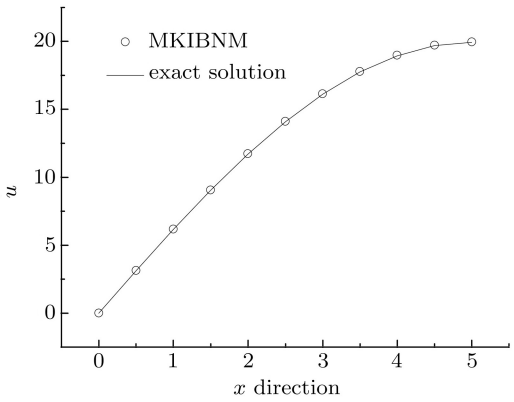

Fig. 7. Exact and numerical solutions of u at $y = 5$.

Numerical results from the MKIBNM, together with the exact solution are shown in Figs. 7 and 8.

Again, the results obtained by the present method match well with the exact solution.

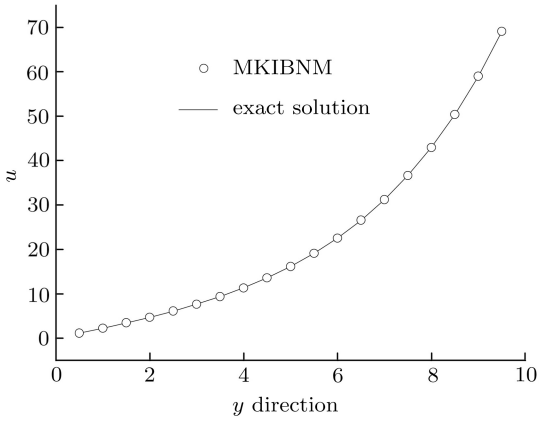

Fig. 8. Exact and numerical solutions of u at $x = 3$.

5. Conclusions

A new formulation of the boundary-type meshfree method, called the MKIBNM, is presented for 2D potential problems. The boundary integral equation is discretized using the moving Kriging interpolation based on scattered nodes on the boundary of the problem domain. The shape functions constructed using the moving Kriging interpolation possess Kronecker's delta property, then the boundary conditions can be imposed easily and directly. The MKIBNM does not require element or mesh for the interpolation of boundary variables, and possesses the dimensionality advantage. In addition, the MKIBNM also has simpler implementation procedures and lower computation cost than the BNM due to simpler interpolation scheme and smaller system equation dimension. The numerical results demonstrate that the present MKIBNM is an effective meshless method.

References

[1] Belytschko T, Krongauz Y, Organ D, Fleming M and Krysl P 1996 *Comput. Methods Appl. Mech. Eng.* **139** 3

[2] Zhang X, Liu Y and Ma S 2009 *Advances in Mechanics* **39** 1 (in Chinese)

[3] Nayroles B, Touzot G and Villon P 1992 *Comput. Mech.* **10** 307

[4] Belytschko T, Lu Y Y and Gu L 1994 *Int. J. Numer. Meth. Eng.* **37** 229

[5] Atluri S N and Zhu T 1998 *Comput. Mech.* **22** 117

[6] Liu G R and Gu Y T 2001 *Int. J. Numer. Meth. Eng.* **50** 937

[7] Cheng Y M and Li J H 2005 *Acta Phys. Sin.* **54** 4463 (in Chinese)

[8] Liew K M and Cheng Y M 2009 *Comp. Meth. Appl. Mech. Eng.* **198** 3925

[9] Chen L and Cheng Y M 2008 *Acta Phys. Sin.* **57** 1 (in Chinese)
[10] Chen L and Cheng Y M 2008 *Acta Phys. Sin.* **57** 6047 (in Chinese)
[11] Zhang J M, Yao Z H and Li H 2002 *Int. J. Numer. Meth. Eng.* **53** 751
[12] Ren H P, Cheng Y M and Zhang W 2009 *Chin. Phys.* B **18** 4065
[13] Cheng Y M and Peng M J 2005 *Sci. Chin.* Ser. G: *Phys. Mech. Astron.* **48** 641
[14] Cheng Y M, Liew K M and Kitipornchai S 2009 *Int. J. Numer. Meth. Eng.* **78** 1258
[15] Peng M J and Cheng Y M 2009 *Eng. Anal. Bound. Elem.* **33** 77
[16] Qin Y X and Cheng Y M 2006 *Acta Phys. Sin.* **55** 3215 (in Chinese)
[17] Cheng Y M and Chen M J 2003 *Acta Mech. Sin.* **35** 181 (in Chinese)
[18] Lancaster P and Salkauskas K 1981 *Math. Comput.* **37** 141
[19] Mukherjee Y X and Mukherjee S 1997 *Int. J. Numer. Meth. Eng.* **40** 797
[20] Kothnur V S, Mukherjee S and Mukherjee Y X 1999 *Int. J. Solids Struc.* **36** 1129
[21] Zhu T, Zhang J D and Atluri S N 1998 *Comput. Mech.* **21** 223
[22] Zhu T, Zhang J and Atluri S N 1998 *Comput. Mech.* **22** 174
[23] Gu L 2003 *Int. J. Numer. Meth. Eng.* **56** 1
[24] Zheng B J and Dai B D 2010 *Acta Phys. Sin.* **59** 5182 (in Chinese)